Topological Confinement and Superconductivity

K. A. Al-Hassanieh,[1] C. D. Batista,[1] P. Sengupta,[1] and A. E. Feiguin[2,3]

[1]*Theoretical Division T-11, Los Alamos National Laboratory, Los Alamos, NM 87545, USA*
[2]*Condensed Matter Theory Center, Department of Physics, The University of Maryland, College Park, MD 20742, USA*
[3]*Microsoft Project Q, The University of California, Santa Barbara, CA 93106, USA*

We derive a Kondo Lattice model with a correlated conduction band from a two-band Hubbard Hamiltonian. This mapping allows us to describe the emergence of a robust pairing mechanism in a model that only contains repulsive interactions. The mechanism is due to topological confinement and results from the interplay between antiferromagnetism and delocalization. By using Density-Matrix-Renormalization-Group (DMRG) we demonstrate that this mechanism leads to dominant superconducting correlations in a 1D-system.

PACS numbers: 74.20.-z, 74.20.Mn, 71.10.-w, 71.10.Fd

The origin of unconventional superconductivity remains as one the most important open problems of condensed matter physics. Physicists do not agree on the mechanism that pairs the electrons to form the superconducting condensate. To a very good approximation, electrons only interact via the repulsive Coulomb interaction. Consequently, as it was pointed out recently by Anderson [1], the crucial question is: "How can this repulsion between electrons be eliminated in favor of electron pair binding?" The problem becomes even more puzzling if we consider that the Coulomb interaction is bigger than the bandwidth for most of the unconventional superconductors. Then, the first challenge is to demonstrate that a "pairing force" can exist in model Hamiltonians that only contain strongly repulsive interactions. Although different pairing mechanisms have been proposed over the last twenty years, it is not always clear if those mechanisms actually work or if they are robust under the presence of long range Coulomb interactions. This is mainly due to the lack of controlled approximations for solving models of strongly interacting electrons in 2D or 3D.

Another aspect that is quite ubiquitous in unconventional superconductors is the proximity of the superconducting state to an antiferromagnetic (AFM) phase. This observation suggests that antiferromagnetic correlations are related to the pairing mechanism. However, although several "magnetic" pairing mechanisms have been proposed [2], it is still unclear how the interplay between AFM correlations and itineracy leads to a "glue" that is strong enough to hold the two electrons together. It is the purpose of this Letter to show how a robust pairing mechanism emerges out of this interplay and to demonstrate that it leads to dominant superconducting correlations in a two-band Hubbard chain. Moreover, we will see that the pairing is still robust in the proximity of the AFM region, i.e., when there are large AFM fluctuations but no AFM order. What makes the mechanism robust is the fact that it is driven by confinement of topological defects (solitons) that are attached to each carrier (holes). In particular, as we will see below, this implies that the binding energy and the size of the pair are determined by different energy scales.

We start by deriving an extended Kondo lattice (KL) chain with a correlated $(t-J)$ conduction band as the low-energy effective model $\tilde{H}$ of the original two-band Hubbard Hamiltonian H. The correlated nature of the conduction band is the main difference with the standard KL chain that was extensively studied in previous works [3]. With a simple analytical treatment of the fully anisotropic (Ising-like) limit of $\tilde{H}$, we show the origin of the two-hole bound state and the corresponding binding energy in the dilute limit. Our DMRG calculations allow us to extend these results to the fully isotropic (Heisenberg) limit and to finite hole concentrations. Moreover, we show that the superconducting pair-pair correlations are the dominant ones over an extended and relevant region of the quantum phase diagram. Interestingly enough, the pairing remains robust in the absence of long-range AFM order (fully isotropic limit) indicating that a long enough AFM correlation length is sufficient for stabilizing the pairing mechanism that we discuss below.

We will consider the following two-band Hubbard chain:

$$\begin{aligned} H \;=&\sum_{j;\sigma;\eta}(e_\eta-\mu)n_{j\sigma\eta}+t_{\eta\eta}(c^\dagger_{j+1\sigma\eta}c_{j\sigma\eta}+c^\dagger_{j\sigma\eta}c_{j+1\sigma\eta}) \\ &+\sum_{j;\sigma}t_{ul}(c^\dagger_{j\sigma u}c_{j\sigma l}+c^\dagger_{j\sigma l}c_{j\sigma u})+\sum_{j;\eta}U_\eta n_{j\uparrow\eta}n_{j\downarrow\eta}, \end{aligned} \quad (1)$$

where $1\leq j\leq L$, L is even, $L+1\equiv 1$ [periodic boundary conditions (PBC)], $\eta=\{l,u\}$ denotes the lower and upper bands, and $\sigma=\{\uparrow,\downarrow\}$. The diagonal energies are $e_u=\Delta_{ul}/2$ and $e_l=-\Delta_{ul}/2$ with $\Delta_{ul}>0$, and the density operators are $n_{j\sigma\eta}=c^\dagger_{j\sigma\eta}c_{j\sigma\eta}$.

From now on, we will assume that the mean number of electrons per unit cell is $1\leq n\leq 2$. For $t_{\eta\eta'}=0$ and $U_u>\Delta_{ul}$, the ground state subspace, $\mathcal{S}$, consists of states containing one electron per site in the lower band (only spin remains as a degree of freedom). In contrast, the sites of the upper band can be empty or singly occupied. In the strong coupling limit, $U_u,U_l,\Delta_{ul}\gg t_{\eta\eta'}$ and $U_l-\Delta_{ul}\gg t_{ul}$, the low-energy spectrum of H is described by the effective Hamiltonian, $\tilde{H}$, that acts on the subspace $\mathcal{S}$ and results from applying degenerate perturbation theory to second order in the hopping terms:

$$\begin{aligned} \tilde{H} \;=&\; t_{uu}\sum_{j;\sigma}(\bar{c}^\dagger_{j+1\sigma u}\bar{c}_{j\sigma u}+\bar{c}^\dagger_{j\sigma u}\bar{c}_{j+1\sigma u})+\sum_{j;\sigma}(e_u-\tilde{\mu})\bar{n}_{j\sigma u} \\ &+\;\sum_{j\nu\eta}J^\nu_\eta S^\nu_{j\eta}S^\nu_{j+1\eta}+\sum_{j\nu}J^\nu_K S^\nu_{ju}S^\nu_{jl}, \end{aligned} \quad (2)$$

where $\bar{c}^{\dagger}_{j\sigma u} = c^{\dagger}_{j\sigma u}(1 - n_{j\bar{\sigma}u})$ (constraint of no double-occupancy), $\nu = \{x, y, z\}$, $J^{\nu}_{\eta} = 4t^2_{\eta\eta}/U_{\eta}$, and $J^{\nu}_{K} = 2t^2_{ul}/(U_l - \Delta_{ul}) + 2t^2_{ul}/(U_u + \Delta_{ul})$. Although the exchange interactions are isotropic ($J^{\nu}_{\eta} = J_{\eta}$ and $J^{\nu}_{K} = J_K$), we split the Heisenberg terms for reasons that will become clear later. Note that we have neglected the attractive, $-\frac{J_u}{4}\bar{n}_j\bar{n}_{j+1}$, and the correlated hopping terms that also appear to second order in t_{uu} to keep $\tilde{H}$ simple and because they are not relevant for the pairing derived below. A more extensive study including the effect of these terms will be presented elsewhere [4]. To simplify the notation, we will introduce $t = t_{uu}$, $J = J^z_u$, $\alpha J = J^x_u = J^y_u$, $J_H = J^z_l$, and $\beta J_H = J^x_l = J^y_l$. Where $0 \leq \alpha, \beta \leq 1$ determine the exchange anisotropies. $\tilde{H}$ is an extension of the Kondo Lattice chain: the localized spins of the lower band are coupled via a Kondo interaction, J_K, to the itinerant electrons of the upper band which are described by a $t - J$ model. In contrast to the usual Kondo Lattice, the itinerant electrons are strongly correlated and the local spins are AFM coupled via J_H.

In the following, we set $t = 1$ as the energy scale and use $J = 0.4$, $J_H = 0.5$. These values correspond for instance to $U_u = 10, U_l = 16$ and $t_{ll} = \sqrt{2}$. We will start by assuming an Ising-like ($\beta = 0$) coupling between the localized spins to stabilize long-range antiferromagnetic order at $T = 0$. The fully isotropic case $\alpha = \beta = 1$ will be considered in the second part of the manuscript, so $\beta = 0$ unless its value is explicitly specified. Below we will drop the band index in the definition of the different correlation functions because they are always applied to the conduction band. We will only compute the ground state properties.

We use the DMRG method [5, 6] to study systems up to 100 unit cells at $T = 0$. The PBC increase substantially the computational effort. In the finite-system step, we keep up to $M = 1400$ states per block and perform up to 12 sweeps. The weight of the discarded states is kept to the order $10^{-6}-10^{-10}$ for $\beta = 0$, and 10^{-5} for $\beta = 1$ [7].

We first consider the simplest case of Ising-like exchange interactions ($\alpha = 0$) and a Kondo coupling much smaller than the rest of the terms in $\tilde{H}$. In this situation, the exchange J_H forces the localized spins to be AFM ordered in the ground state. For the $J_K = 0$ ground state, each hole added to the conduction band carries a soliton or anti-phase domain wall (ADW) for the AFM order parameter [8]. For $J_K \neq 0$, the single hole quasiparticle becomes a spinon-holon bound state [see Fig.1(a)] to avoid an energy increase of order LJ_K [9]. The single added hole is topologically neutral: the holon and the spinon carry solitons with opposite "charge" (kink and anti-kink). We also note that unless the spinon and the holon are on the same site, the ferromagnetic link associated to the spinon increases the magnetic energy by $J/2$. This provides an additional attractive force between the spinon and the holon. In this fully anisotropic limit, the spinon is immobile and the holon is localized around it [10].

The situation is qualitatively different for the two-hole ground state [see Fig.1(b)]. The spinons attached to each

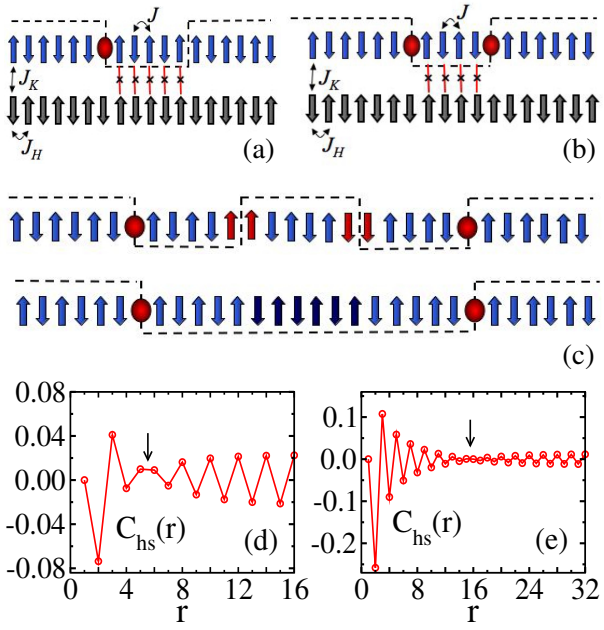

FIG. 1: (Color online) (a) Scheme of the single-hole quasiparticle. The holon and spinon carry solitons with opposite topological charges as indicated by the dashed line. The itinerant and localized spins are ferromagnetically aligned between the holon and spinon leading to a string or confining (linear) potential. (b) Scheme of the two-hole ground state. The holons carry solitons with opposite charge and are bound together by a magnetic string. (c) Formation of holon-holon bound state from two free holes. The two spinons with opposite spins and topological charges cancel each other, leaving two holons with opposite topological charges attached by the string. (d) $C_{hs}(r)$ for a single hole. The arrow indicates the position of the spinon. (e) $C_{hs}(r)$ for two holes with $\alpha = 1.0$, $J_K = 0.05$, and $L = 100$. The reference holon is at $r = 1$. The arrow indicates the position of the second holon. Each holon carries an ADW as explained in the text.

holon cancel each other (they have opposite spins and topological charges) leading to a bound state of two holons attached by a magnetic string. The cancellation of the two spinons lowers the magnetic energy by $\sim J$. Consequently, we expect the two-holon bound state to be more stable than two independent spinon-holon pairs. This statement can be quantified by computing the exact ground state energies for one and two holes (this can be done for $\alpha = 0$ because the spins are not exchanged by $\tilde{H}$). In particular, for $J_K = 0.1$, we get a binding energy $\Delta_B = E_g(N_h) + E_g(N_h - 2) - 2E_g(N_h - 1) \simeq -0.25$ for $N_h = 2$, where $E_g(N_h)$ is the ground state energy for N_h holes. The holon-holon pair formation is illustrated in Fig.1(c). The mutual cancellation of the two spinons leaves the two holons attached by a magnetic string.

This simple picture for one and two holes has been discussed previously in the context of a $t - J$ model in a staggered magnetic field [11]. In our case, the staggered magnetic field h is not artificial because it is self-generated by the AFM ordering of the localized spins. As it was pointed out in [11], the limit $h \to 0$ ($J_K \to 0$ in our case) is singular: $\lim_{h\to 0}\Delta_B = -J$ while the mean distance between the two holes diverges as $h^{-1/3}$ ($J_K^{-1/3}$). This singular behavior is a

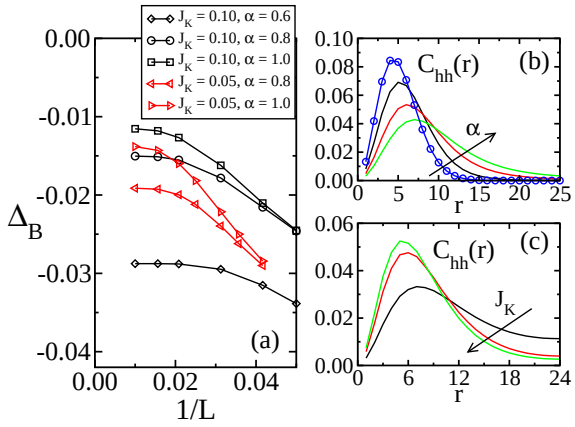

FIG. 2: (Color online) (a) Finite size scaling of Δ_B. The results indicate robust pairing in the thermodynamic limit for for all values of α. (b) Density-density correlation function $C_{hh}(r)$ for $J_K = 0.1$ and $\alpha = 0.0, 0.6, 0.8$, and 1.0. C_{hh} clearly confirms the existence of a holon-holon bound state. Exact results are shown in open circles for the Ising limit ($\alpha = 0$) and the agreement with DMRG is excellent. (c) $C_{hh}(r)$ in the fully isotropic limit ($\alpha = \beta = 1$) for $J_K = 0.2, 0.3$, and 0.35. A bound state is formed in this limit.

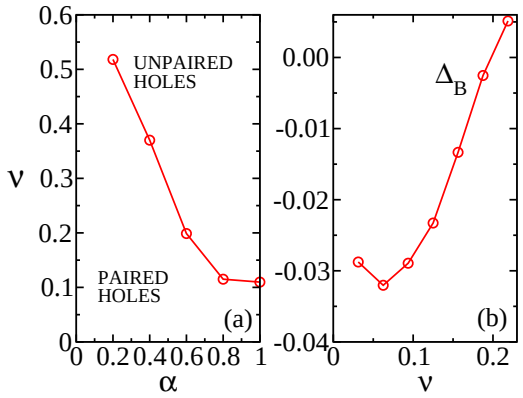

FIG. 3: (Color online) (a) (α, ν) phase diagram for $L = 64$ and $J_K = 0.1$. Near the Ising limit ($\alpha = 0.2$), the pairing survives up to $\nu \approx 0.5$ ($N_h \approx 32$). For a given α, the boundary between the two phases is determined from the condition $\Delta_B(\alpha, \nu_c) = 0$ with ν_c being the lowest value of ν which satisfies this condition (holes are not bound for $\nu > \nu_c$). (b) $\Delta_B(\nu)$ for $\alpha = 0.6$. In the thermodynamic limit ($L \to \infty$), Δ_B should be zero for $\nu > \nu_c$; however $\Delta_B(L = 64) > 0$ due to finite size effects.

manifestation of the qualitative difference between the single- and two-hole states: *the binding energy Δ_B and the size of the two-holon bound state, l_p, are determined by two independent energy scales*. While $\Delta_B \sim -J$ for small enough h (J_K), l_p only depends on h (J_K) as long as J is nonzero. In particular, this shows that a negative binding energy, $\Delta_B < 0$, does not imply the formation of a two-hole bound state. The negative value of Δ_B for $h \to 0$ ($J_K \to 0$) just indicates that a single hole always creates a spinon [see Fig.1(a)] while this is not true for the two-hole state as shown in Figs.1(b) and (c). An infinitesimal field h (J_K) is enough for stabilizing the bound state due to the topological nature of the two-hole state: each hole carries a soliton and the two solitons become confined for any finite h. This remarkable property makes the pairing robust against the inclusion of a more realistic longer range Coulomb interaction in H. We will see below that this pairing mechanism survives in the absence of long range AFM order, i.e., when the effect of the localized spins *cannot* be replaced by a staggered mean field h because $\langle \mathbf{S}_{i\eta} \rangle = 0$. This is a very important qualitative difference relative to the case considered in [11].

The above picture remains valid away from the Ising limit ($\alpha > 0$). However, the hole can now move coherently in one sublattice. The process involves the exchange of the two spins on adjacent nearest and next-nearest neighbor sites of the hole via the αJ term followed by two hoppings in the same direction. This coherent motion of the hole leaves the magnetic background unchanged. For $0 \leq \alpha \leq 1$, the holon and spinon form a bound state. The magnetic structure of this quasiparticle is shown schematically in Fig. 1(a). To confirm the above picture, we compute the hole-spin correlation function $C_{hs}(r) = \langle S^z_i n^h_{i+1} S^z_{i+r} \rangle$, where $n^h_j = 1 - (n_{j\uparrow} + n_{j\downarrow})$ is the hole density at site j. Figure 1(d) shows $C_{hs}(r)$ in the isotropic limit ($\alpha = 1$) with one hole in the conduction band. The correlator shows the spinon (indicated by the arrow) separated from the holon (at $r = 1$) by a finite distance. C_{hs} shows clearly that the holon and spinon carry an ADW. When a second hole is added to the conduction band, the spinons cancel each other, as explained above, leaving the two holons attached to ADW's of opposite sign. This is also confirmed by the calculation of C_{hs} [see Fig. 1(e)]. The reference holon is at $r = 1$ while the average position of the second holon is indicated by the arrow (note that this average distance is artificially increased due to the PBC). To the left side of the second holon, the spins at even numbered sites ($r = 2$ for example) are antiparallel to the reference spin; whereas to its right, they are parallel (e.g. $r = 32$).

In the following we present numerical evidence of pairing and dominant superconducting correlations as a function of hole density $\nu = N_h/L$. Figure 2(a) shows the pairing energy $\Delta_B = E_g(2) + E_g(0) - 2E_g(1)$ in the dilute limit $\nu \to 0$ versus $1/L$ and for different values of J_K and α. The finite size scaling of Δ_B shows robust pairing in the thermodynamic limit for all values of α. Figure 2(b) shows the density-density correlation function $C_{hh}(r) = \langle n^h_i n^h_{i+r} \rangle$ for $J_K = 0.1$ and different values of α. C_{hh} shows a clear maximum at a finite distance confirming that the two holons are bound. As expected, the distance between the two holons increases with α. In the Ising limit, $\alpha = 0$, the DMRG results are compared to the exact solution and the agreement is excellent.

So far we have only considered the limit $\beta = 0$ because the pairing mechanism is easier to identify in the presence of long-range AFM order. It is natural to ask if the pairing survives in the fully isotropic limit ($\alpha = \beta = 1$) relevant for our original Hamiltonian H. In the absence of holes, the ground state of $\tilde{H}$ only exhibits short-range AFM correlations due to the gap induced by the relevant J_K coupling. The C_{hh} correlator for the two-hole ground state shown in Fig.2(c) provides clear evidence of the formation of a two-hole bound state. Moreover, the pair size l_p decreases monotonically with increasing J_K (slope of the confining potential) indicating that the pairing mechanism remains the same.

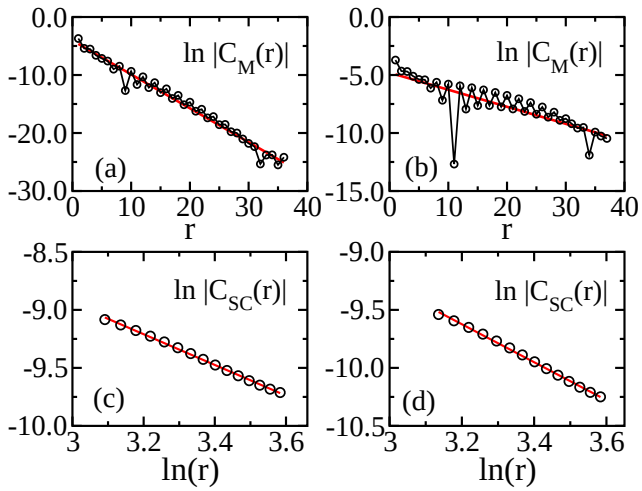

FIG. 4: (Color online) Single particle, C_M, and pair-pair, C_{SC}, correlation functions. The circles show the numerical results, and the straight lines show the best fit. (a), (c) $J_K = 0.05$, $\alpha = 0.2$. (b), (d) $J_K = 0.05$, $\alpha = 0.6$. $C_M(r)$ shows an exponential decay whereas $C_{SC}(r)$ shows a power law decay. This confirms the emergence of dominant superconducting correlations.

For finite hole concentration, a new length scale $1/\nu$, that is the mean distance between holes, appears in the problem. We expect the previous analysis of the dilute limit to remain valid as long as $l_p \ll 1/\nu$. On the other hand, the pairing should be suppressed when the these two lengths become comparable because the effective interaction between holes is repulsive at short distances. This expectation is fully consistent with the numerical results shown in Fig.3. The boundary between the paired and unpaired regions (see Fig.3a) is shifted to lower hole concentrations when α gets closer to one, i.e., when l_p becomes bigger. In particular, Fig.3b shows the evolution of the pairing energy Δ_B as a function of ν for $\alpha = 0.6$. Δ_B ceases to be negative for a hole concentration close to 20% ($\nu_c \sim 0.2$). This implies that if we vary the chemical potential, the states with odd number of holes are metastable as long as $\nu < \nu_c$. We note that the critical hole concentration ν_c remains significantly high ($\nu_c \sim 0.1$) in the limit $\alpha = 1$.

To confirm the presence of dominant superconducting correlations, we compare the single particle $C_M(r) = \sum_\sigma \langle \bar{c}_{i+r\sigma} \bar{c}^\dagger_{i\sigma} \rangle$ and pair-pair $C_{SC}(r) = \langle \Delta_{i+r} \Delta^\dagger_i \rangle$ correlation functions, with $\Delta^\dagger_i = \frac{1}{\sqrt{2}} (\bar{c}^\dagger_{i+1\uparrow} \bar{c}^\dagger_{i\downarrow} - \bar{c}^\dagger_{i+1\downarrow} \bar{c}^\dagger_{i\uparrow})$. Figure 4 shows results obtained for $L = 80$, $N_h = 4$, $J_K = 0.05$ and $\alpha = 0.2, 0.6$. The single particle correlator decays exponentially while the pair-pair correlator shows a slower algebraic decay. The exponential decay of the single particle correlator is due to the fact that holes are bound in pairs. In the dilute limit, the probability of finding the two holes separated by a distance r bigger than the pair size l_p (see Fig.2b) decreases exponentially in r. The algebraic decay of $C_{SC}(r)$ is expected for a Luttinger liquid of pairs. The comparison between $C_M(r)$ and $C_{SC}(r)$ clearly indicates that the ground state has dominant superconducting correlations in the regime under consideration.

A few comments are in order. We verified that the pairing ($\Delta_B < 0$) persists for smaller values of J_H such as $J_H = J_K = 0.1$. The small J_H regime of $\tilde{H}$ is relevant for describing lanthanide and actinide based compounds in which localized f-electrons interact via Kondo exchange with electrons in the conduction band. Conduction bands with strong $3d$-character are correlated and would provide a natural realization of our $\tilde{H}$. If the $t-J$ conduction band of $\tilde{H}$ is replaced by the original Hubbard upper band of H, one can study the evolution of our pairing mechanism as a function of U_u/t (the standard KL model is recovered for $U_u/t = 0$) [4].

In contrast to pairing mechanisms driven by an attractive short range interaction (like the AFM exchange J), our mechanism is robust under the inclusion of a more realistic longer range Coulomb interaction. This results from the fact that Δ_B and l_p are determined by two independent energy scales (J and J_K). In other words, a big enough value l_p reduces the effect of longer range Coulomb terms without reducing the value of Δ_B (note that l_p and Δ_B are anticorrelated when the pairing is produced by a short range attractive potential).

Finally, our pairing mechanism should also persist for weakly coupled chains (small inter-chain hopping) due to its topological nature. While single-particle coherent inter-chain hopping is not possible due to the soliton that is attached to each hole, a pair can hop coherently between chains because it is topologically neutral (soliton-antisoliton bound state). Such coherent pair-hopping should stabilize a superconducting state below a finite critical temperature. A detailed study of this extension to higher-dimensional systems will be presented elsewhere [4].

The authors thank E. Dagotto, J. Bonca, S. Trugman, U. Schollwöck, G. Martins, and C. Büsser for helpful discussions. LANL is supported by the U.S. DOE under Contract No. W-7405-ENG-36.

[1] P. W. Anderson, Science **317**, 1705 (2007).
[2] E. Dagotto, Rev. Mod. Phys. **66**, 763 (1994).
[3] H. Tsunetsugu, *et al.*, Rev. Mod. Phys. **69**, 809 (1997); I. P. McCulloch, *et al.*, Phys. Rev. B **65**, 052410 (2002); D. J. Garcia, *et al.*, Phys. Rev. Lett. **93**, 177204 (2004); J. C. Xavier and E. Dagotto, Phys. Rev. Lett. **100**, 146403 (2008).
[4] K. A. Al-Hassanieh et al, to be publised.
[5] S. R. White, Phys. Rev. Lett. **69**, 2863 (1992); Phys. Rev. B **48**, 10345 (1993).
[6] K. Hallberg, Adv. Phys. **55**, 477 (2006); U. Schollwöck, Rev. Mod. Phys. **77**, 259 (2005).
[7] To get good accuracy for this model, it is useful to keep a large number of states in the infinite-system DMRG step and to consider each unit cell as one lattice site with 2×3 states.
[8] C. D. Batista and G. Ortiz, Phys. Rev. Lett. **85**, 4755 (2000).
[9] This confining mechanism is analogous to the one that binds spinons in pairs (magnons) when a finite coupling between AFM chains is turned on.
[10] J. Smakov *et al.*, Phys. Rev. Lett. **98**, 266401 (2007).
[11] J. Bonca *et al.*, Phys. Rev. Lett. **69**, 526 (1992); P. Prelovsek *et al.*, Phys. Rev. B **47**, 12224 (1993).